

Theoretical stability of a perfect thorium crystal subjected to multidirectional stresses

K. P. Thakur

*Department of Physics, Tej Narayan Banaili College, Bhagalpur University,
Bhagalpur 812 007, India*

(Received 24 February 1982; revised manuscript received 3 May 1982)

A theoretical study is made of the lattice stability or theoretical strength of thorium subjected to various kinds of simple stresses. Calculations are carried out with the use of generalized Morse potential and the stability criterion of Born. The region of G , M , and S stability of thorium in the $a_2=a_3$ plane of the a_1, a_2, a_3 space is investigated. Many simple cases of lattice deformation arise as specific cases of the generalized calculations presented here. A wealth of data for various elastic moduli, internal energy, and stresses throughout a wide range of lattice deformation is presented. This study indicates the presence of a stress-free bcc phase of thorium, which has a cell length of 4.04 Å, in close agreement with the experimental observation. We have found two internal-energy minima corresponding to the stress-free fcc and bcc phases. The path of phase transformation (fcc→bcc) in thorium is predicted on the basis of the present study.

I. INTRODUCTION

The prediction of the theoretical strength of a solid is of fundamental interest since it represents an upper bound to the actual strength of the solid and some metallic whiskers approach the theoretical limit. The study of theoretical strength is of considerable interest in systems where substantial elastic deformation may occur. The elastic deformation may be large and nonlinear in a variety of circumstances, particularly if (i) it is highly localized (i.e., near the cracks or other structures that increase stress), (ii) the deformed specimen is very small (e.g., whiskers or integrated-circuit structures), or (iii) it occurs very rapidly (e.g., in mechanical twinning, shock loading, or martensitic phase transformations). Hill¹ pointed out that "single crystals free from lattice imperfections are used increasingly as microstructural components. Perfect crystals are capable of elastic strains well beyond what can properly be treated as infinitesimal. Their response to general loading is virtually unknown and is doubtless complex, so experimentation will have to be conducted within some plausible theoretical framework."

The importance of this study in several phenomena of metallurgy, solid-state physics, solid mechanics, and geophysics attracted the interest of several investigators since Born² first began this investigation in 1940. Recent studies, mostly carried out by Milstein *et al.*,³ revealed many interesting behaviors of solids under stress (not all of which could have been anticipated beforehand). Still,

there exists a need for an extensive study to uncover the behavior of stressed solids. We studied^{4,5} the theoretical strength of nickel subjected to multidirectional stresses ($\sigma_1 \neq \sigma_2 = \sigma_3$) corresponding to the lattice deformation in the $a_2=a_3$ plane of the a_1, a_2, a_3 space. Our generalized calculation generates the cases of many simple modes of loading.

In this paper we report the theoretical stability of thorium subjected to multidirectional stresses ($\sigma_1 \neq \sigma_2 = \sigma_3$). The element Th is selected because (i) it obeys the Cauchy condition $C_{12} = C_{44}$ more closely than Ni (the ratio C_{12}/C_{44} is 0.94 for Th and 1.145 for Ni), (ii) it exhibits^{6,7} a phase transformation (fcc→bcc) at 1636 K with a transition enthalpy of 2.72 kJ mol⁻¹, and (iii) in the bcc phase the cell length of thorium is $b = 4.11 \pm 0.01$ Å.^{8,9} Thus it will be very interesting to find the extent to which our study can explain the existence of a stress-free state in the bcc phase, which is experimentally observed. Moreover, thorium is an important metal for nuclear scientists, and it will be of interest to study its stability and general behavior under multidirectional stresses.

II. THEORETICAL APPROACH

A. Crystal model

In order to perform computations of load, strain, and elastic moduli, a crystal model is required for computing the internal energy W per atom as a

function of geometric variables q_r ($r = 1, 2, \dots, 6$) that define the state of homogeneous strain of the crystal

$$W = W(q_1, q_2, \dots, q_6). \quad (1)$$

The internal energy W is taken as a pairwise sum of interactions $\phi(r)$ over a large number of atoms in the lattice to obtain convergence up to the desired significant figures.

Milstein¹⁰ suggested a generalized Morse function

$$\phi_m(r) = \frac{D}{m-1} \{ \exp[-m\alpha(r-r_0)] - m \exp[-\alpha(r-r_0)] \}, \quad (2)$$

where D , α , r_0 , and m are potential parameters, $d\phi/dr = 0$ at $r = r_0$, and $\phi(r_0) = -D$, the dissociation energy of two atoms. The generalized Morse function (2) with m between 1.25 and 6 has certain inherent theoretical advantages.^{3,10} The Morse function results from setting $m = 2$ in the generalized equation (2).

We have carried out the computations of the P - V behavior¹¹ of Th using different members of the generalized Morse family (2) and found that (i) the result does not vary much with m , and (ii) the computed values agree fairly well with the shock-wave data of McQueen and Marsh.¹² For the present study we confine ourselves to $m = 6$ in the generalized Morse model; some interesting results for $m = 1.25$ in family (2) has also been reported since it would provide some information on the role of the nature of the details of the function ϕ_m . Our justification for performing the present computations within the framework of this simplified model is that, apparently, such computations have not heretofore been carried out for thorium.

Furthermore, our experience^{4,5,11} and the studies of Milstein^{3,10,13-15} indicated that much of the qualitative or semiquantitative, computed, path-dependent behavior is mainly a result of crystal geometry or symmetry and is therefore, for the most part, model independent. Included in the family of the generalized Morse function ϕ_m are both short-range steep functions and long-range shallow functions. The effects of varying m on the shape and properties of function (2) have been studied by Milstein¹⁰ and Huang *et al.*¹⁴

In view of these considerations, calculations in the present study are carried out using two "extreme" members of the generalized Morse family with $m = 1.25$ and 6, corresponding to the "shallowest" as well as "steepest" potentials. Surpris-

ingly, both members gave almost similar results for thorium (to be discussed in the following sections).

B. Computation procedure

For computational purposes it is convenient to define a set of lattice vectors that remain mutually orthogonal along the axisymmetric path, and thereby constitute the edges of an orthorhombic cell. In the present study we consider the general case of loading such that

$$a_1 \neq a_2 = a_3, \quad \sigma_1 \neq \sigma_2 = \sigma_3, \quad (3)$$

which corresponds to deformation in the $a_2 = a_3$ plane of the a_1, a_2, a_3 space.

A lattice vector \vec{r} connecting the origin atom with any other site in the crystal is given by

$$\vec{r} = \frac{1}{2}(m_1 \vec{a}_1 + m_2 \vec{a}_2 + m_3 \vec{a}_3), \quad (4)$$

where \vec{a}_i represents vectors coincident with the edges of either a fc or bc cell; if the fc cell is chosen as reference, the m_i are integers such that $m_1 + m_2 + m_3$ is even; if the reference cell is bc, the m_i are all even or all odd integers at any lattice site, and a_i represent the cell lengths, i.e., magnitude of vectors \vec{a}_i .

A computer program that selects the allowed indices m_1 , m_2 , and m_3 relative to the axes of the orthorhombic cell is used to evaluate the following lattice summations, considering a sufficiently large number of atoms in the lattice to ensure convergence up to five significant figures:

$$W = \frac{1}{2} \sum_{m_1} \sum_{m_2} \sum_{m_3} \phi_m(r^2), \quad (5)$$

$$s_i = \sum_{m_1} \sum_{m_2} \sum_{m_3} \frac{d\phi_m(r^2)}{d(r^2)}, \quad (6)$$

and

$$S_{ijkl} = \sum_{m_1} \sum_{m_2} \sum_{m_3} m_i m_j m_k m_l \frac{d^2 \phi_m(r^2)}{[d(r^2)]^2}. \quad (7)$$

The load F_i acting along the a_i direction on the face of the unit cell is given by

$$F_i = N \frac{dW}{da_i} = \frac{N}{4} a_i s_i, \quad (8)$$

where N is the number of atoms per unit cell (4 for fc and 2 for bc). The Cauchy or true stress is then

$$\sigma_i = \frac{F_i}{a_j a_k}. \quad (9)$$

III. CRITERIA OF STABILITY

In what is popularly known as the "Born stability criterion," positive definiteness of the current matrix of elastic moduli,

$$C_{rs} = \frac{\partial^2 W}{\partial q_r \partial q_s}, \quad (10)$$

is taken to be synonymous with stability, where q_r ($r=1, 2, \dots, 6$) are generalized coordinates, namely, geometric variables that define the homogeneous strain of the crystal. For cubic crystals under multidirectional stresses defined by Eq. (3), the Born criterion leads to the well-known conditions

$$\begin{aligned} C_{22} - C_{23} &> 0, \\ C_{22} + C_{23} - 2(C_{12}^2)/C_{11} &> 0, \\ C_{44} &> 0, \\ C_{55} &> 0. \end{aligned} \quad (11)$$

This is important to note that in a crystal under load, convexity of the internal-energy function is not coordinate invariant, as pointed out by Hill.¹ Hence, the conditions (11) are thoroughly "relative" in the sense that they are dependent upon the choice of the geometric variables. Milstein and Hill¹⁶ studied the stability of cubic crystals under hydrostatic loading for the complete family of the generalized Morse functions using three different geometric variables, and they confirmed the findings of Hill that convexity of internal-energy depends upon the choice of geometric variables. Milstein and Farber,¹⁷ and Milstein, Hill, and Huang¹⁸ also find divergencies among the domains of Born stability for different choices of q_r . Various choices of q_r will give the same results at the stress-free reference state. Hence it is certain all of these different choices will generate almost similar results near the stress-free state of the crystal.

IV. G , M , AND S MODULI

Three sets of the elastic moduli C_{rs} leading to three different choices of strain measure have been favored in the literature.¹⁹ The set of Green moduli represented by C_{rs}^G is used by investigators who follow the Born method,²⁰ using components of the Green tensor for the generalized coordinates q_r . The set of S moduli, C_{rs}^S , is the choice of Macmillan and Kelly²¹ and is generated using the elements of the stretch tensor for q_r . The set of Milstein moduli, C_{rs}^M , is generated by using edges of

the deformed cell and their included angles for q_r .

With the selection of the unstressed fcc thorium as the reference state, the Green moduli at any stage of loading can be evaluated¹ from

$$C_{ijkl}^G = \frac{Na_i^0 a_j^0 a_k^0 a_l^0}{8a_1^0 a_2^0 a_3^0} S_{ijkl}, \quad (12)$$

where a superscript 0 designates the reference state and the four-index—tensor notation, C_{ijkl} , is usually represented²⁰ by two-index matrix notation, C_{rs} , after the indices are contracted as $(ij) \rightarrow r$, and $(kl) \rightarrow s$, according to the scheme $(11) \rightarrow 1$, $(22) \rightarrow 2$, $(33) \rightarrow 3$, $(23) \rightarrow 4$, $(31) \rightarrow 5$, and $(12) \rightarrow 6$.

On any orthorhombic path from which a bc or fc cell can be defined, the elastic moduli relative to the M and S variables are readily evaluated from transformation formulas developed by Hill and Milstein.¹⁹ For the M moduli,

$$C_{ijjj}^M = \lambda_i \lambda_j C_{ijjj}^G + \delta_{ij} l_i / \lambda_i, \quad (13)$$

$$C_{ijkl}^M = \lambda_i \lambda_j \lambda_k \lambda_l C_{ijkl}^G \quad (i \neq j, k \neq l). \quad (14)$$

For the S moduli,

$$C_{ijjj}^S = C_{ijjj}^M, \quad (15)$$

$$\begin{aligned} C_{ijik}^S = \frac{1}{4}(\lambda_i + \lambda_j)(\lambda_i + \lambda_k) C_{ijik}^G \\ + \frac{1}{4} \delta_{kj} (l_i / \lambda_i + l_j / \lambda_j) \quad (i \neq j, i \neq k), \end{aligned} \quad (16)$$

where δ_{ij} is the Kronecker delta, l_i is the force per unit reference area acting along the a_i direction, and $\lambda_i = a_i / a_i^0$.

V. RESULTS AND DISCUSSION

A. Potential parameters

The input data for fcc thorium are $a_0 = 5.0612$ Å, $C_{11} = 0.779 \times 10^{12}$ dyn cm⁻², $C_{12} = 0.482 \times 10^{12}$ dyn cm⁻², and $C_{44} = 0.513 \times 10^{12}$ dyn cm⁻², taken from Konti and Varshni²² where the original sources are given. The values of potential parameters calculated using the method suggested by Milstein¹⁰ are listed in Table I.

Our approach to determine the range of stability, the modes of lattice failure of the crystal, is to compute the internal energy, W , the stresses $\sigma_1, \sigma_2, \sigma_3$ ($\sigma_2 = \sigma_3$ in the present case), and the elastic moduli C_{rs}^G , C_{rs}^M , and C_{rs}^S as a function of lattice deformation defined by Eq. (3). After computing

TABLE I. Values of the potential parameters of the generalized Morse potential (2) for fcc thorium obtained by the method developed by Milstein (Ref. 10).

m	α (\AA^{-1})	r_0 (\AA)	D (10^{-12} erg)
1.25	1.876 455	3.666 237	0.430 451
6.00	0.583 239	4.021 494	0.282 993

the values of the elastic moduli, we apply the Born criterion (11) to find out whether the crystal is stable in the current state of loading or not. The GHOST subroutine in a Burroughs 6700 machine was used to obtain the graphical output of all the results, which are presented here in graphical form for the lattice deformation defined by Eq. (3), corresponding to the deformation in the $a_2=a_3$ plane of the a_1, a_2, a_3 space.

The results presented here are given according to the generalized Morse function (2) with $m=6$, apart from a few interesting cases where results are also quoted for $m=1.25$ for comparison; ultimately, we find that the results do not greatly depend on the choice of m in the generalized Morse function (2).

Figure 1 shows two unit cells of the fct lattice having sides a_1, a_2 , and a_3 with specific atoms shown with solid centers to indicate that the structure could also be considered as a bct having sides b_1, b_2 , and b_3 . In Fig. 1

$$b_1=a_1, \quad b_2=b_3=a_2/2^{1/2}=a_3/2^{1/2}, \quad (17)$$

since the present case of lattice deformation is specified by Eq. (3).

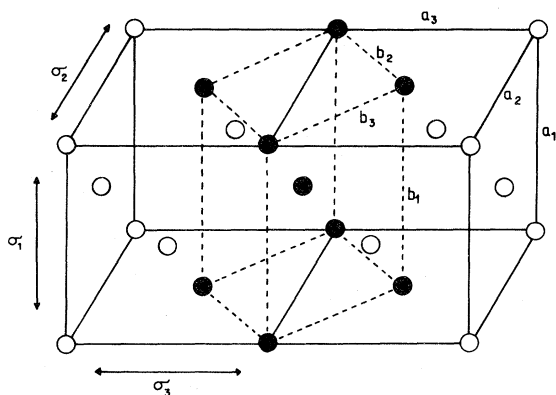


FIG. 1. Two unit cells of fct lattice with specific lattice sites shown with "solid centers" to indicate the bct unit cell. This figure also indicates the direction of applied multidirectional stresses.

For the fcc phase of the crystal, we have

$$a_1=a_2=a_3 \quad (18)$$

whereas for the bcc phase, we have

$$b_1=b_2=b_3, \quad 2^{1/2}a_1=a_2=a_3. \quad (19)$$

The directions of the applied multidirectional stresses $\sigma_1, \sigma_2, \sigma_3$ (in the present study $|\sigma_2|=|\sigma_3|$) are also indicated in Fig. 1.

B. Stresses

Figures 2 and 3, respectively, present the contours of σ_1 and $\sigma_2 (= \sigma_3)$ in the $a_2=a_3$ plane of the a_1, a_2, a_3 space. The hydrostatic stresses working on the crystal is specified by the condition

$$\sigma_1=\sigma_2=\sigma_3, \quad (20)$$

which specifies the path obtained from the locus of the points of intersection of contours of same heights in Figs. 2 and 3. These figures show the presence of three such cases of hydrostatic pressure corresponding to (i) the fcc phase specified by Eq. (18), (ii) the bcc phase specified by Eq. (19), and (iii) a bct phase close to the bcc phase. The contours of $\sigma_1=0$ in Fig. 2 and $\sigma_2=\sigma_3=0$ in Fig. 3 intersect each other at $a_1=a_2=a_3=a_0$, indicating, obviously, the stress-free fcc phase of thorium. However, these contours are tangent up to a considerable range of lattice deformation near the bcc phase in between $a_1=3.90 \text{ \AA}$, $a_2=a_3=5.80$

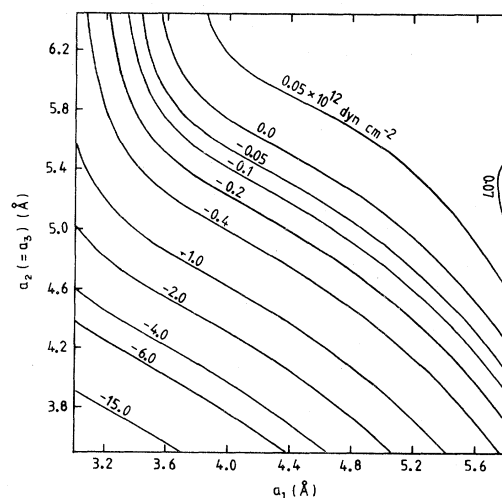


FIG. 2. Contours of σ_1 in the $a_2=a_3$ plane of the a_1, a_2, a_3 space for thorium according to the generalized Morse function (2) with $m=6$.

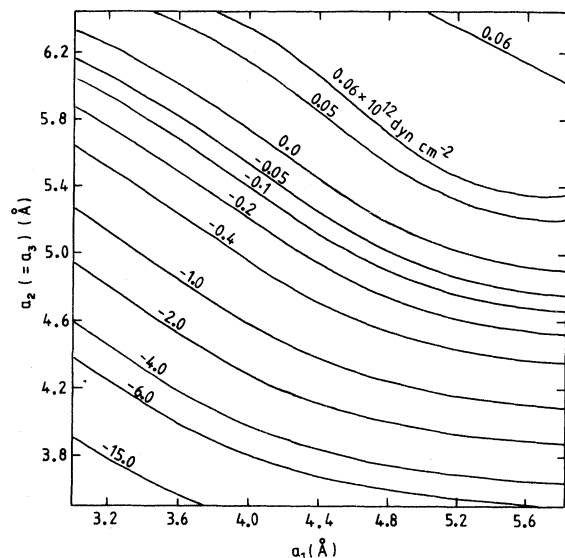


FIG. 3. Contours of $\sigma_2 (= \sigma_3)$ in the $a_2 = a_3$ plane of the a_1, a_2, a_3 space for thorium according to the generalized Morse function (2) with $m = 6$.

Å, and $a_1 = 4.07$ Å, $a_2 = a_3 = 5.67$ Å. The stress-free bcc phase is thus found at $a_1 = 4.04$ Å, $a_2 = a_3 = 5.71$ Å, corresponding to $b_1 = b_2 = b_3 = 4.04$ Å. Figures 2 and 3 give an indication of the amount of stresses required to carry out any deformation of the lattice in the $a_2 = a_3$ plane of the a_1, a_2, a_3 space.

C. Internal energy

Figure 4 shows the contours of energy per unit cell, E , in the $a_2 = a_3$ plane of the a_1, a_2, a_3 space. This figure also indicates the positions of the stress-free fcc phase (solid circle) and the stress-free bcc phase (circle), which lie, respectively, in the principal internal-energy minimum and secondary minimum.

The potential energy surface of thorium under deformation is shown in Fig. 5. This figure also indicates the presence of the principal minimum at the stress-free fcc phase of the crystal and a secondary minimum in the bcc phase. Figures 4 and 5 show that the potential energy increases very slowly as we pass from the stress-free fcc phase to the stress-free bcc phase near the path traced by the $\sigma_2 = \sigma_3 = 0$ contour (in Fig. 3). The potential barrier between the two potential wells is very small, of the order of 0.2×10^{-12} erg, smaller than the similar barrier height for nickel.^{4,5}

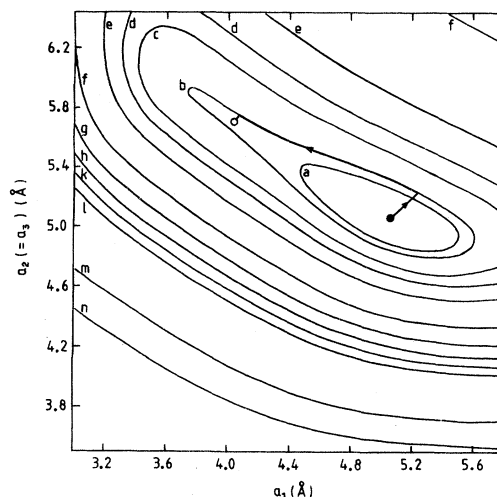


FIG. 4. Contours of the internal energy per unit cell of thorium in the $a_2 = a_3$ plane of the a_1, a_2, a_3 space according to the generalized Morse function (2) with $m = 6$. This figure also indicates the points \bullet , corresponding to the principal minimum in the fcc phase and \circ , corresponding to the secondary minimum in the bcc phase. The path of phase transformation (fcc \rightarrow bcc) is also indicated in this figure. The contour heights in 10^{-12} erg are a, -17.2 ; b, -17.0 ; c, -16.5 ; d, -16.0 ; e, -15.0 ; f, -12.0 ; g, -9.0 ; h, -6.0 ; k, -3.0 ; l, -0.0 ; m, 30.00 ; n, 60.00 .

D. Elastic moduli

The elastic moduli C_{rs}^G , C_{rs}^M , and C_{rs}^S are calculated for thorium under the deformation specified by Eq. (3) according to the method discussed in Sec.

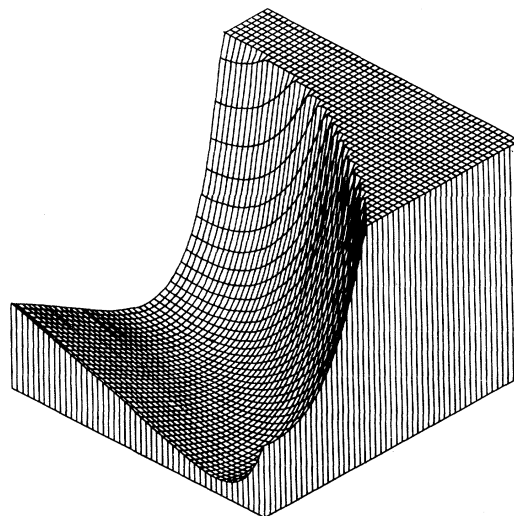


FIG. 5. Potential energy surface in the $a_2 = a_3$ plane of the a_1, a_2, a_3 space for thorium according to the generalized Morse function (2) with $m = 6$.

IV, using the generalized Morse potential (2) with two extreme values of m . The contours of these elastic moduli have been plotted in the $a_2 = a_3$ plane of the a_1, a_2, a_3 space. These figures are not included in this paper; however, they are available from the author.

With the Morse model, or whenever the strain energy comes solely from pairwise interactions, it is known¹ that the tensor of the Green moduli, C_{rs}^G , always possesses the "Cauchy symmetry," regardless of the reference configuration for the strain, in the sense that

$$C_{23}^G = C_{44}^G, \quad C_{12}^G = C_{55}^G$$

for any choice of coordinate axes.

The present results for the elastic moduli indicate that

$$C_{11}^G = C_{22}^G, \quad C_{12}^G = C_{23}^G,$$

$$C_{11}^M = C_{22}^M, \quad C_{12}^M = C_{23}^M, \quad C_{44}^M = C_{55}^M,$$

and

$$C_{11}^S = C_{22}^S, \quad C_{12}^S = C_{23}^S, \quad C_{44}^S = C_{55}^S$$

is true for the fcc lattice under hydrostatic compressive and tensile stresses.

E. Stability ranges

In order to obtain the ranges of lattice stability, we must find whether the elastic moduli, calculated in Sec. VD, satisfy the Born criteria (11) or not. The quantities

$$C_a = C_{22} - C_{23}$$

and

$$C_b = C_{22} + C_{23} - 2(C_{12})^2/C_{11}$$

that appear in the inequality criteria (11) have been plotted for G , M , and S moduli (these figures are not included here and can be obtained from the author).

According to criteria (11), the boundary of the G stable region is specified by the contours of zero heights of $C_{12}^G (= C_{55}^G)$, $C_{23}^G (= C_{44}^G)$, C_a^G , and C_b^G . The area under which thorium is stable with respect to G under deformation specified by Eq. (3) is shown in Fig. 6, obtained according to the generalized Morse function (2) with $m = 6$.

The boundary of the region that is stable with respect to M is specified by the contours of zero heights of C_{44}^M , C_{55}^M , C_a^M , and C_b^M , whereas the

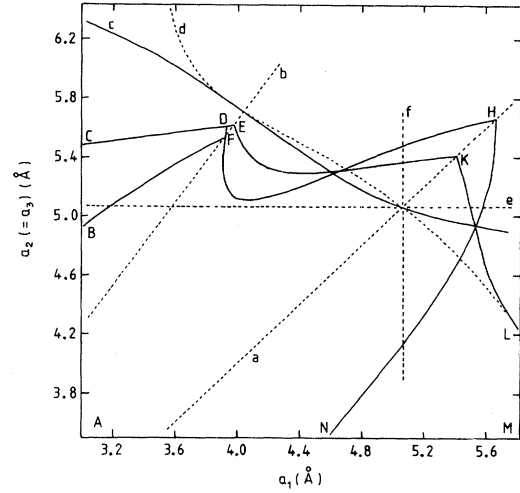


FIG. 6. Region of G , M , and S stability of thorium in the $a_2 = a_3$ plane of the a_1, a_2, a_3 space according to the generalized Morse function (2) with $m = 6$. This figure also includes the lines and curves showing a , the fcc phase of the lattice under hydrostatic compressive and tensile stresses; b , the bcc phase of the lattice under hydrostatic compressive and tensile stresses; c , the lattice under unidirectional stress; d , the lattice under two-directional stresses; e , the lattice under unidirectional deformation; f , the lattice under two-directional deformation. The specification of various curves and stable areas are given in Table II.

boundary of areas that are stable with respect to S in the $a_2 = a_3$ plane of the a_1, a_2, a_3 space is specified by the contours of zero heights of C_{44}^S , C_{55}^S , C_a^S , and C_b^S . The areas stable with respect to M and S thus obtained are shown in Fig. 6.

Figure 6 also includes lines and curves that demonstrate the following. a is the fcc phase of the lattice under hydrostatic compressive or tensile stresses defined by Eq. (18). b is the bcc phase of the lattice under hydrostatic compressive or tensile stresses defined by Eq. (19). c is the lattice under unidirectional stress ($\sigma_2 = \sigma_3 = 0$, in this case the only stress acting upon the crystal is σ_1 , due to which a_1 changes; at the same time a_2 and a_3 simultaneously relax to make $\sigma_2 = \sigma_3 = 0$). d is the lattice under two-directional stresses ($\sigma_1 = 0$, $\sigma_2 = \sigma_3$; in this case, equal amount of stresses act along a_2 and a_3 directions, and the lattice relaxes to make $\sigma_1 = 0$). e is the unidirectional deformation of the crystal (in this case, $a_2 = a_3 = a_0$, and a_1 changes). f is the two-directional deformation of the lattice (in this case, $a_1 = a_0$; a_2 and a_3 change simultaneously by equal amount).

The results of the calculation of the stability range of thorium according to the generalized

Morse potential (2) with $m = 1.25$ are shown in Fig. 7. Computed values of stresses σ_i ($i = 1, 2, 3$) and internal energy do not vary much with the choice of m in the generalized Morse function (2). All members of the Morse family (2) give exactly the same result for the stress-free bcc phase of the crystal, which is certainly independent of the choice of m in the generalized Morse function (2). In Figs. 6 and 7, curves d and c are tangent up to a considerable range of lattice deformation near the bcc phase, indicating the presence of a stress-free state in that range apart from one in the fcc phase, where curves d and c intersect each other. Figures 6 and 7 indicate that the stability range changes slightly with the choice of m in function (2). The specification of various curves in Figs. 6 and 7 is given in Table II. The only thing that changes with the choice of m in function (2) is the stability range and hence the elastic moduli, as indicated by Figs. 6 and 7.

F. Phase transformation

Figures 6 and 7 indicate that the $\sigma_1 = 0$ contour (curve d) and the $\sigma_2 = \sigma_3 = 0$ contour (curve c) intersect at $a_1 = 4.04$ Å, $a_2 = a_3 = 5.71$ Å on line b , representing the presence of the stress-free bcc phase of the crystal with cell lengths (in bcc phase) $b_1 = b_2 = b_3 = 4.04$ Å. Figures 4 and 5 also support the presence of a secondary internal energy minimum at this point in the bcc phase, having a barrier height of the order of 2×10^{-13} erg per unit fcc cell. Thus from these results one would expect that thorium should exist in the bcc phase with a cell length of 4.04 Å.

Surprisingly, thorium does show^{6,7} a phase

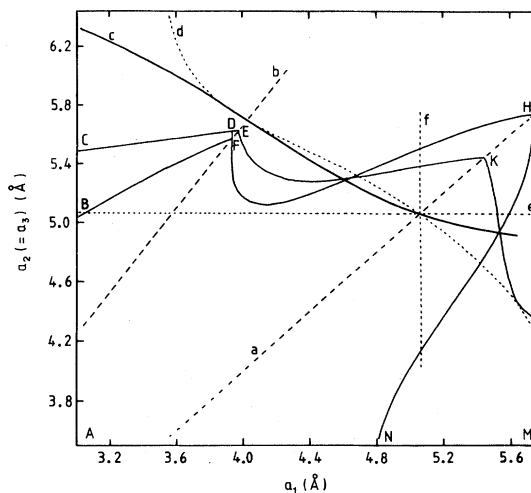


FIG. 7. Same as Fig. 6 but with $m = 1.25$ in the generalized Morse function (2).

transformation (fcc \rightarrow bcc) at 1636 K with transition enthalpy of 2.72 kJ mol⁻¹. The cell length for bcc thorium^{8,9} measured at 1450 °C is $b = 4.11 \pm 0.01$ Å, in a close agreement with $b = 4.04$ Å, obtained from the results of this study. This in itself offers us encouragement to present our results.

In this study, the stresses σ_i , internal energy E , and the elastic moduli C_{rs} are independently calculated as functions of lattice deformation (i.e., changes in cell lengths a_1, a_2, a_3), regardless of the methods of these changes. The application of hydrostatic pressure to a fcc crystal will move the system "downwards" on line a , Figs. 6 and 7, from the stress-free fcc phase (i.e., the cell lengths a_1, a_2, a_3 will keep decreasing by equal amount). On the other hand, increasing the temperature of

TABLE II. Specification of various curves in Figs. 6 and 7.

Curves	Contours of zero value of quantities	Boundary of stability type
CDE	$C_{23}^G, C_{44}^G, C_{23}^M, C_{44}^M$	G stable, M stable
BF	C_{44}^S	S stable
EK	C_b^G	G stable
KL	C_a^G	G stable
DFH	C_b^M, C_b^S	M stable, S stable
HN	C_a^M, C_a^S	M stable, S stable
ABCDEKLMNA		G-stable area
ABCDFHNA		M-stable area
ABFHNA		S-stable area

the crystal will move the system "upwards" on line a , Figs. 6 and 7, and cell lengths a_1, a_2, a_3 will keep increasing by equal amount. Thus the application of high temperature to the crystal corresponds to the application of a hydrostatic tensile stress. Extrapolating the thermal expansion data²³ of thorium (available only up to 800 K), we find that at 1636 K, the temperature of phase transformation (fcc→bcc), thorium should possess the cell lengths of $a_1 = a_2 = a_3 = a = 5.23 \text{ \AA}$, in its fcc phase. It is very interesting to note in Fig. 4 that at $a = 5.23 \text{ \AA}$, the internal-energy contours just start circulating around both fcc and bcc minima, whereas at $a_0 < a < 5.23 \text{ \AA}$, the contours keep circulating only around the principal minimum of the fcc phase, preventing the phase transition at a lower temperature (in the range of lattice deformation $a_0 < a < 5.23 \text{ \AA}$). The amount of tensile hydrostatic stress required to create a lattice deformation equivalent to that from heating the crystal to 1636 K (i.e., to change the cell lengths from a_0 to 5.23 \AA), estimated from Figs. 2 and 3, is of the order of $4 \times 10^{11} \text{ dyn cm}^{-2}$. Our current technology is not so developed to apply hydrostatic tensile stress of this order of magnitude to verify whether or not we can get a phase transition in thorium without heating it to a high temperature.

The path of phase transformation (fcc→bcc) in thorium could be obtained from the above-mentioned consideration where cell lengths of the crystal in its fcc phase will change from a_0 to 5.23 \AA by heating it to 1636 K. At $a = 5.23 \text{ \AA}$, the internal-energy contour circulates around both fcc and bcc minima (Fig. 4), which will bring the crystal from fcc to bcc phase without changing its internal energy. This path of phase transformation in thorium is indicated in Fig. 4. The barrier height between the stress-free fcc and bcc phases is of the order of $2 \times 10^{-13} \text{ erg per unit fcc cell}$, which corresponds to the transition enthalpy of 3 kJ mol^{-1} , in good agreement with the observed transition^{5,6} enthalpy of 2.72 kJ mol^{-1} .

The only thing that inhibits the phase transformation is the stability range; the crystal appears to be unstable in the stress-free bcc phase (Figs. 6 and 7). However, the crystal is stable in the bcc phase under hydrostatic compressive stress (Figs. 6 and 7), stable with respect to G in the range $b \leq 3.977 \text{ \AA}$, stable with respect to M and S in the range $b \leq 3.937 \text{ \AA}$. Here we must recall (see Hill¹) that the stability range depends upon the choice of geometric variables q_r , and we should see if there exist other choices of q_r , according to Hill's criterion, that can show the stability of the stress-free

bcc phase of thorium.

Another reason for not observing the G , M , and S stability in the stress-free bcc phase could be the fact that the Morse potential (or any other two-body atomic potential) is not applicable to the bcc crystals.¹⁰ According to the results of the stability region in Figs. 6 and 7, one can obtain many other paths of phase transformation inside the stability region; any line joining the equilibrium point in the fcc phase to curve b inside the stability region will show the possible path of phase transformation (fcc→bcc). Unidirectional deformation in the crystal is one of such possible paths in which different amount of stresses will be required along different cell lengths ($\sigma_1 \neq \sigma_2 = \sigma_3$), which is not possible in actual practice. Moreover, the bcc phase thus obtained would not be stress-free.

VI. SUMMARY AND CONCLUSION

While commenting on the results, we should note that our work is the first in which a theoretical range of lattice stability of thorium has been revealed in a plane; no attempt has been made so far to study the stability of thorium in any mode of loading. Included in this study are calculations of the variations, throughout a wide range of applied stresses, in all lattice parameters, the stresses σ_i , internal energy E , elastic moduli $C_{rs}^G, C_{rs}^M, C_{rs}^S$, and the stability relations expressed in terms of C_{rs} . Wealth of data for various elastic moduli throughout a wide range of lattice deformation enables us to assess the strength of thorium under multidirectional stresses.

Unfortunately, there are no experimental or theoretical data currently sufficient for any metal involving various modes of lattice failure to substantiate the present results for the lattice stability. However, the successful prediction of the stress-free bcc phase of thorium in this paper supports the validity of the generalized Morse functions for the description of the mechanical properties of fcc metals and also produces the testimony of our approach for the study of the behavior of solids under multidirectional stresses. In passing, one can note that the present approach is the first one in which the actual path of phase transformation in a metal is revealed. These calculations indicate what is actually going on in the crystal that is subjected to multidirectional stresses.

ACKNOWLEDGMENT

The author thanks Professor F. Milstein of the University of California, Santa Barbara for his

generous help in carrying out these calculations. The interest and comments given by Professor R. Hill, of the University of Cambridge are very much appreciated and gratefully acknowledged.

-
- ¹R. Hill, *Math. Proc. Camb. Philos. Soc.* **77**, 225 (1975).
²M. Born, *Proc. Camb. Philos. Soc.* **36**, 160 (1940).
³F. Milstein, in *Mechanics of Solids*, The Rodney Hill 60th Anniversary Volume, edited by H. G. Hopkins and M. J. Swell (Pergamon, Oxford, 1981), and references therein.
⁴K. P. Thakur and H. D. B. Jenkins, *J. Phys. F* **10**, 1925 (1980).
⁵K. P. Thakur, *J. Appl. Phys.* (in press).
⁶R. R. Hultgren, R. L. Orr, P. D. Anderson, and K. K. Kelley, *Selected Values of Thermodynamic Properties of Metals and Alloys* (Wiley, New York, 1963), and supplements.
⁷D. D. Wagman, T. L. Jobe, E. S. Domalski, and R. H. Schumm, in *American Institute of Physics Handbook*, 3rd ed., edited by D. E. Gray (McGraw-Hill, New York, 1972).
⁸W. B. Pearson, *Handbook of Lattice Spacing and Structures of Metals and Alloys* (Pergamon, New York, 1967).
⁹J. D. H. Donnay, W. P. Mason, and E. A. Wood, in *American Institute of Physics Handbook*, Ref. 7.
¹⁰F. Milstein, *J. Appl. Phys.* **44**, 3825 (1973); **44**, 3833 (1973).
¹¹K. P. Thakur, D. Sc. thesis, University of Allahabad, India, 1982 (unpublished).
¹²R. G. McQueen and S. P. Marsh, *J. Appl. Phys.* **31**, 1253 (1960).
¹³F. Milstein, *Phys. Rev. B* **3**, 1130 (1971).
¹⁴K. Huang, F. Milstein, and J. A. Baldwin, Jr., *Phys. Rev. B* **10**, 3635 (1974).
¹⁵F. Milstein and K. Huang, *Phys. Rev. B* **18**, 2529 (1978).
¹⁶F. Milstein and R. Hill, *J. Mech. Phys. Solids* **25**, 457 (1977); **26**, 213 (1978); **27**, 255 (1979).
¹⁷F. Milstein and B. Farber, *Phys. Rev. Lett.* **44**, 277 (1980).
¹⁸F. Milstein, R. Hill, and K. Huang, *Phys. Rev. B* **21**, 4282 (1980).
¹⁹R. Hill and F. Milstein, *Phys. Rev. B* **15**, 3087 (1977).
²⁰M. Born and R. Fürth, *Proc. Camb. Philos. Soc.* **36**, 454 (1940).
²¹N. H. Macmillan and A. Kelly, *Mater. Sci. Eng.* **12**, 79 (1973); *Proc. R. Soc. London* **330**, 309 (1972).
²²A. Konti and Y. P. Varshni, *Can. J. Phys.* **47**, 2021 (1969).
²³R. K. Kirby, T. A. Hans, and B. D. Rothrock, in *American Institute of Physics Handbook*, Ref. 7.